Eur Biophys J (1997) 26: 155–162

ARTICLE

Marie-Odile Roy · Jonas Uppenberg
Stéphane Robert · Mireille Boyer · Joël Chopineau
Magali Jullien

Crystallization of monoacylated proteins: influence of acyl chain length

Received: 4 October 1996 / Accepted: 13 December 1996

Abstract The crystallization of monoacylated proteins has been investigated using a model system. Acylated derivatives of bovine pancreatic ribonuclease A, differing in their acyl chain lengths (10 to 16 carbon atoms), have been prepared using reverse micelles as microreactors. With one fatty acid moiety per polypeptide chain, covalently attached to the NH_2 terminus of the protein, all the modified proteins have similar enzymatic activity and hydrodynamic radius as the native protein. Only the caprylated derivative can give crystals which diffract to high resolution. The resolved structure indicates that: (i) the protein folding is not modified by the chemical modification, (ii) the capryl moiety is not buried within the molecule but available for external interactions. Dynamic light scattering experiments on concentrated solutions show that protein-protein interactions are dependent on acyl chain length. Proteins with the longest attached chains (14 and 16 carbon atoms) tend to self-associate through acyl group interactions.

Key words Acylation · Ribonuclease A · Self-association · Protein crystallography · Dynamic light scattering

Abbreviations AOT bis(2-ethylhexyl)sodium sulfosuccinate · ARF ADP-ribosylation factor · cAPK cAMP-dependent protein kinase · 2′,3′-CMP cytidine 2′:3′-phosphate · ESI-MS electrospray ionization mass spectroscopy · GDP · guanosine 5′-diphosphate · GTP guanosine 5′-triphosphate · HPLC high-performance liquid chromatography · Mega-8 octanoyl-N-methylglucamide · NNLS Non-Negatively-constrained Least Squares · RNase A bovine pancreatic ribonuclease A

M.-O. Roy · J. Uppenberg · M. Boyer · M. Jullien (✉)
Centre de Biochimie Structurale, CNRS UMR C9955,
Université Montpellier I, INSERM U414, Faculté de Pharmacie,
15, avenue Charles Flahault, F-34060 Montpellier Cedex, France
(Fax: 33 04 67 52 96 23; e-mail: jullien@tome.cbs.univ-montpl.fr)

S. Robert · J. Chopineau
Laboratoire de Technologie Enzymatique,
UPRES CNRS A6022, Université de Technologie de Compiègne,
BP 529, F-60205 Compiègne Cedex, France

Introduction

The growth of high-quality crystals remains a bottleneck in determining atomic structures from X-ray crystallography. This is particularly true for integral membrane proteins since only a handful of such structures, as compared to thousands for soluble proteins, have been determined to date. The major difficulty in the crystallization of membrane proteins comes from the specific features of their surfaces: a significant portion is hydrophobic and buried in the bilayer core. Thus, membrane proteins are not truly soluble in water and cannot alone form the isotropic, monodisperse solutions needed to grow crystals; the heterogeneous natural lipids from the membrane must be replaced by a homogeneous detergent environment (Garavito and Picot 1990).

Whereas the process by which soluble proteins crystallize has received considerable attention in recent years (McPherson 1995), less effort has been directed to membrane proteins. One way to investigate the crystallization process in relation to membrane proteins, is to focus on protein surface properties. In this paper, we address how the addition of hydrophobic groups on the surface of a soluble protein may modify its solubility and interfere with its crystallization.

Acylation is one of the modifications by which soluble proteins can obtain hydrophobic groups on their surface. Three general classes of lipidation can be distinguished: N-myristoylation at the N-terminus, S-prenylation at or near the C-terminus and S-palmitoylation. The corresponding fatty acyl groups contain 14 to 20 carbons. Involved in transmembrane signaling (Casey 1995), acylated proteins include the well-known trimeric G-proteins which serve to link receptors exposed at the cell surface to intracellular effectors such as enzymes and ion channels, the small

G protein superfamily, protein kinases and a variety of viral proteins. It is now established that the lipids attached to these signalling molecules play crucial roles in their functions through either lipid-lipid based hydrophobic interactions or lipid-protein interactions (Marshall 1993).

Acylated proteins are difficult to produce in such quantities that permit the study of their crystallization process. Here, the effect of acylation on crystallization is investigated by using a chemically modified protein as a model system. Acyl groups with chain lengths of 10, 14 and 16 carbon atoms have been covalently attached to bovine pancreatic ribonuclease A (RNase A) using reverse micelles as microreactors (Kabanov et al. 1989). The acyl group is linked to the N-terminal of the protein. Both protein folding and activity are unchanged by the modification, while solubility and crystallization are affected; above a critical length for the lipid moiety, the acylated protein undergoes self-association which impedes its three-dimensional crystallization.

Material and methods

Chemicals

Bovine pancreatic RNase A was purchased from Boehringer. Capryl chloride, myristoyl chloride, palmitoyl chloride, bis(2-ethylhexyl) sodium sulfosuccinate (AOT) and octanoyl-N-methylglucamide (Mega-8) were from Sigma. Acetonitrile and trifluoroacetic acid, both HPLC grade, were obtained from Fluka. All other reagents were of analytical grade.

Preparation, purification and characterization of acylated ribonucleases

All fatty acid acylations were performed in AOT reverse micelles (0.1 M AOT in isooctane), as previously described (Robert et al. 1993), using molar ratios (water)/(surfactant) = 7 and (reagent)/(protein) = 4. The protein fraction was precipitated by cold acetone, recovered in water and lyophilized. The modified protein was purified using a Si C18 Delta Pak (300 Å, 7.8×300 mm) high-performance liquid chromatography column. Protein elution was achieved by employing an acetonitrile-water (with 0.1% trifluoroacetic acid) gradient elution mode with a flow rate of 3 ml/min. After removal of acetonitrile by evaporation, the protein was lyophilized. The purity of each fraction was checked by analytical HPLC and capillary electrophoresis.

The extent of chemical modification was determined by electrospray ionization mass spectroscopy (ESI-MS), using a Finnegan SSQ710 mass spectrometer equipped with an electrospray inlet system. The instrument was used in the positive mode. Spectra were recorded in the 1000–1900 m/z range in steps of 0.1 m/z with a 2 ms dwell time and with a resolution of 1 Da.

Assignment of chemical modification was deduced from N-terminal sequence analysis; automated Edman degradations were performed with an Applied Biosystems model 477A pulsed liquid protein sequencer system.

Enzymatic activities toward 2′,3′-CMP were determined from the change in absorbance at 292 nm (Crook et al. 1960).

The total average yield of pure modified RNase A was usually about 20% of the starting material.

Crystallization

Crystallization assays were performed by vapor diffusion using the hanging drop method. Crystals of caprylated RNase A were obtained under 3M NaCl and 8% saturated ammonium sulfate in 50 mM acetate buffer (pH 5.1) at 20 °C. The conditions were similar to those previously used for a fluorescent derivative of RNase A (Baudet-Nessler et al. 1993), except that the ammonium sulfate concentration was 8% saturation instead of 20% for the fluorescent derivative. The crystal morphologies were also similar. Crystallization assays of myristoylated and palmitoylated RNase A did not succeed until a detergent was added; among the various assays in the presence of detergents, only 0.25% octanoyl-N-methylglucamide (Mega-8) added to 3 M NaCl, 1% ammonium sulfate led to crystals, but they were small and looked different from the previous ones. Protein homogeneity in all crystals was checked by reverse phase HPLC.

X-ray data collection, processing and structure refinement

Diffraction data were collected with a Mar research image plate, using a Rigaku rotating anode as an X-ray source. Only crystals of caprylated RNase A showed diffraction patterns. A data set to 2.4 Å resolution was collected. The completeness was 96% of all possible reflections in the range 30–2.4 Å, with an R-merge of 6.2%.

The diffraction images were processed with the XDS software (Kabsch 1988). The refinement was carried out with X-PLOR (Brünger 1992). The fluorescent derivative of RNase A refined to 1.7 Å (entry 1RAS of the Protein Data Bank) was used as a starting model (Baudet-Nessler et al. 1993). Since the N-terminal lysine was absent in this model, it was added using the PDB-entry 1RTA as a template. Positional refinement by energy minimization was carried out followed by B-factor refinement, where the backbone atoms and side chain atoms were grouped for each amino acid residue. The 100 water molecules with the lowest B-factor in the original model were kept. The final R-factor for all reflections in the range 8.0–2.4 Å was 18.6% and the free R-factor was 23%. $2F_{obs}–F_{calc}$ and $F_{obs}–F_{calc}$ electron density maps were inspected with the O molecular graphics program (Jones and Kjeldgaard 1992). The crystallographic data are summarized in Table 1.

Table 1 Crystallographic data

Data collection	
Space group:	$P3_221$
Cell dimensions (Å):	a = b = 65.2 c = 65.6
Nr of observations:	15227
Nr of unique reflections:	6302
Resolution of data (Å):	30–2.4
Highest resolution shell:	2.8–2.4
Completeness (%):	96 (97)[a]
R_{merge}[b] (%):	6.2 (19.5)
Structure refinement	
Resolution of data (Å):	7.5–2.4
Highest resolution shell:	2.51–2.40
R-factor[c] (%):	18.6 (24.2)
Free R-factor[c] (%):	23.0 (23.0)
Deviations from ideality[d]:	
Bond lengths (Å):	0.007
Bond angles:	1.4°
Dihedrals:	25.8°
Impropers:	1.2°
Average B-factors (Å^2):	
Main chain atoms:	25.1
Side chain atoms:	32.6
Waters:	45.5

[a] Values in parentheses denote highest resolution shell
[b] $R_{merge} = \Sigma_i\Sigma_j(|I_{ij}-\langle I_i\rangle|)/\Sigma_i\Sigma_j|I_{ij}|$, where I is the intensity, i is an index for all unique reflections, and j is an index for all observations of a unique reflection
[c] R-factor $= \Sigma_h||F_{obs}|-|F_{calc}||/\Sigma_h|F_{obs}|$, where F_{obs} and F_{calc} are the observed and calculated structure factors, respectively. The free R-factor has the same definition but is calculated for a subset of reflections not used in the refinement
[d] Values for the final model as calculated by X-PLOR

Light scattering experiments

Dynamic light scattering experiments were performed using a Brookhaven Instrument, as previously described (Boyer et al. 1996). The temporal correlations of the scattering intensity fluctuations, which are related to the Brownian motion of the solute, are used for determining the translational diffusion coefficient D of the protein. Diffusivity depends on direct and indirect, such as hydrodynamic interactions. In the dilute approximation, D can be written:

$$D = D_0 (1 + ac),$$

where c is the weight protein concentration, a, an interaction parameter and D_0 is related to the hydrodynamic particle diameter d via the Stokes-Einstein relation

$$D_0 = k_bT/3\pi\eta d,$$

with k_b = Boltzmann constant, T = absolute temperature, η = solvent viscosity. Repulsive interactions lead to an increase of D with concentration, while for attractive interactions D decreases with concentrations (Pusey and Tough 1985).

In order to characterize size distributions, two programs provided by Brookhaven Instruments were used for analyzing autocorrelation data. The method of cumulants (Koppel 1972), based on the formalism of the statistical cumulant generating function, proceeds by expanding the field autocorrelation function. It is mostly used to obtain, from the first cumulant, a z-average diffusion coefficient:

$$D = \Sigma I_iD_i/\Sigma I_i,$$

where D_i is the diffusion coefficient of species i and I_i the scattered light intensity of species i, and, from the normalized second cumulant, a polydispersity index. As the polydispersity increases, such series expansion is valid only for small values of delay times. This kind of analysis was performed with the beginning of the autocorrelation curve, the correlator working in the linear mode with twenty equally spaced channels. The Non-Negatively-constrained Least Squares (NNLS) method (Morrison et al. 1985) calculates intensity weighted particle size distribution by inversion of the Laplace transform. This kind of analysis was performed on the complete autocorrelation curve recorded with the correlator working in the ratio mode and with long experiment duration to reduce the noise level. Since the final results were very sensitive to small differences in baseline estimates, only curves obtained with calculated and measured baselines differing by less than 0.1% were considered.

Protein solutions at the desired concentration were prepared by dissolving lyophilized protein in 50 mM acetate buffer, pH 5.1. Before use, the solutions were filtered twice using Millipore filters (Millex-GV4, 0.22 μm filter unit) to remove any dust particles. Sample cells were made of NMR tubes especially shortened for light scattering experiments.

Results

Chemical characterization of the derivatives

Three types of acylation were performed with either decanoic, myristic or palmitic acid chlorides. After acylation, reverse phase HPLC of the protein product always yielded two major fractions (Fig. 1), which exhibited similar enzymatic activities. For each of the three reactions, ESI-MS were performed on both peaks. The mass spectra of all samples were consistent with the presence of two major molecular species containing either 0 or 1 phosphate (or sulfate) group non-covalently bound to the protein and probably located in its active site (Camilleri et al. 1993). The first eluted peak was identified as unmodified RNase A (later called control RNase A in the text) and the second one as acylated RNase A with one acyl group per protein molecule.

N-terminal sequencing using the classical Edman procedure was performed on control and acylated derivatives and the yields of N-terminal lysine were compared. The almost complete absence of chemical degradation for each of the three acylated derivatives compared to the control RNase A indicates that the binding of the single acyl chain occurs at the α-amino group of the N-terminal lysine, since

the Edman degradation reaction cannot proceed without a free NH_2 group.

Crystal structure of caprylated RNase A

The caprylated RNase A crystallizes under salt conditions similar to those used for the native protein (Zegers et al. 1994) and several derivatives (De Mel et al. 1992, Baudet-Nessler et al. 1993). The space group and the unit cell parameters (Table 1) are also similar. Therefore, caprylation does not seem to interfere with the crystallization process. On the contrary, myristoylated and palmitoylated RNases A give crystals only when the detergent Mega-8 is added; these crystals are not suitable for X-ray crystallography since they do not give any diffraction pattern.

Crystallization of caprylated RNase A allowed the conformation of modified RNase A to be determined. An atomic model of a fluorescent derivative of RNase A was refined against a data set collected to 2.4 Å resolution. The average rms deviation from the initial model is 0.235 Å for the α-carbons and 0.370 Å for all non-hydrogen atoms (Fig. 2). It can be concluded that the backbone structure of decanyl-RNase A is the same as fluorescent RNase A. The chemical modification of the terminal lysine has no long-range effects on the conformation of the polypeptide.

Examination of crystal packing reveals a main-chain to main-chain hydrogen bond pairing Lys-1 to Gln-101 of a neighboring molecule (Fig. 3), as in other trigonal crystals of the same space group. The added capryl chain does not interfere with crystal packing. However, the size of the cavity generated by crystal packing in the vicinity of the hydrogen bond appears to be large enough to accommodate a capryl chain. Inspection of the electron density maps did not show any identifiable density for the fatty acid on the modified N-terminal lysine backbone nitrogen.

Mean diffusion coefficients; dependence on protein concentration

Concentrated protein solutions were examined by dynamic light scattering. Analyses with the cumulants method were

Fig. 1 *Top*: HPLC purification of myristoylated RNase A. Approximately 10 mg of protein were applied to a Si C18 Delta Pak column; protein was eluted with a linear gradient of acetonitrile (dotted line), in 0.1% trifluoroacetic acid, over 60 min (flow rate of 3 ml/min). Protein elution was monitored by absorbance at 280 nm. *Bottom*: mass spectra of peak 1 (*left*) and peak 2 (*right*) in Daltons

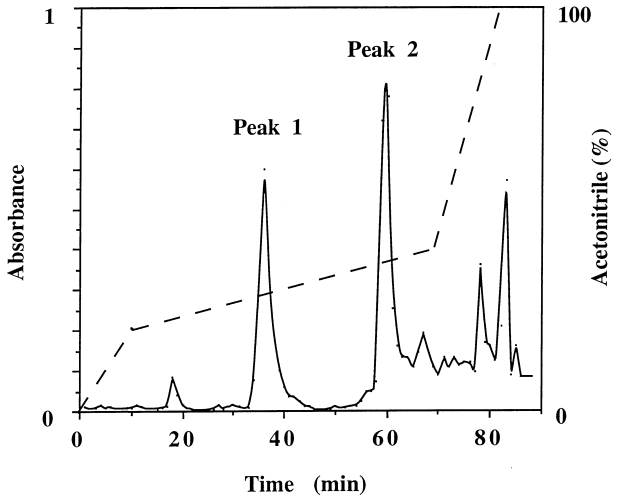

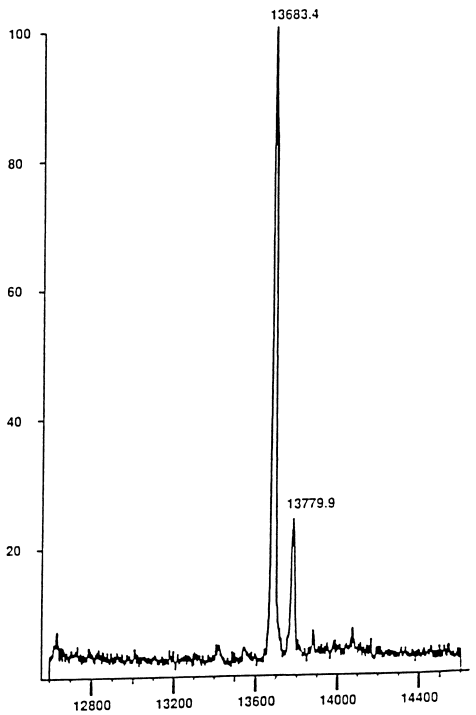

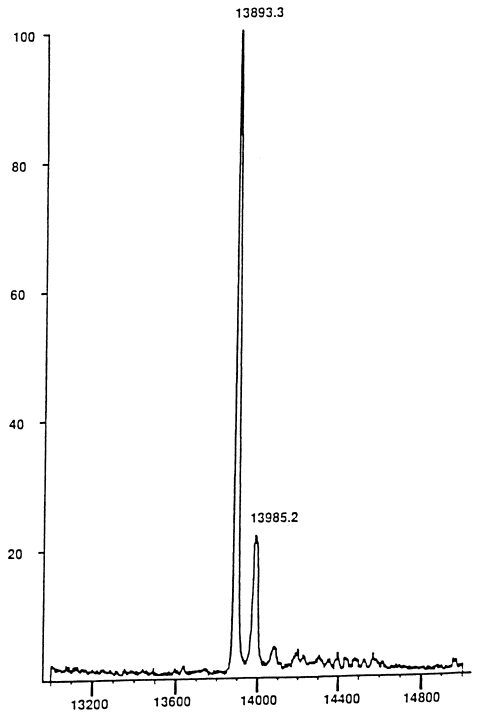

used to study the effect of protein concentration on the diffusion coefficient and calculate an equivalent hydrodynamic diameter. The values of the diffusion coefficient D and polydispersity index as functions of protein concentration are plotted in Fig. 4 for unmodified and acylated ribonucleases. For native (or control) RNase A, at pH 5.1, in the absence of salts, the polydispersity index is small (<0.2) and D is not significantly affected by protein concentration; from extrapolation of D to infinite dilution a hydrodynamic diameter of 4 nm is calculated. For caprylated RNase A, the polydispersity index is also small (<0.2). D decreases linearly as protein concentration increases, indicating attractive interactions. The hydrodynamic diameter calculated from the extrapolated value is similar to that obtained for native protein. For myristoylated and palmitoylated RNases, D also decreases as protein concentration increases, but in contrast to the shorter acyl chain, D values are smaller, corresponding to higher apparent diameters than those observed for native and caprylated RNases. Also, polydispersity indices are very high and increase with protein concentration. These results indicate that the solutions are polydisperse and that myristoylated and palmitoylated proteins probably self-associate in the experimental concentration range.

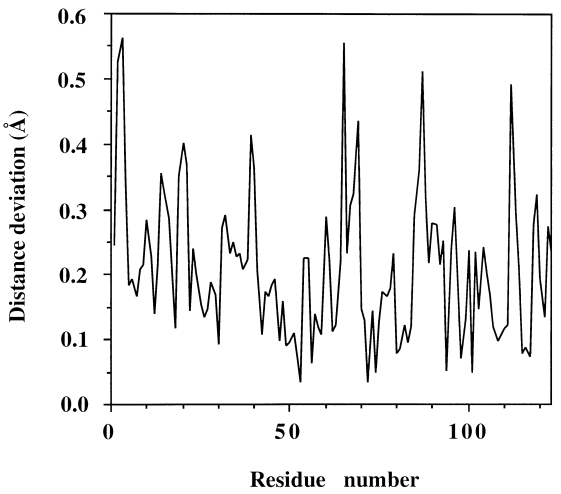

Fig. 2 Distance deviations in Ångströms between the carbon-alpha atoms of the initial model and the refined caprylated RNase model as a function of residue number

Fig. 3 Environment of the N-terminal lysine in the trigonal crystal form. The bottom of the figure shows the residues Lys-1, Glu-2 and Thr-3. The top of the figure shows two regions of a neighbouring molecule (residues 19–23 on the left and 99–102 on the right). An intermolecular hydrogen bond exists between the backbone nitrogen of Lys-1 and the carbonyl oxygen of Gln-101. The caprylation of this nitrogen does not necessarily interfere with the hydrogen bond and there are no packing constraints, other than the ones shown, that hinder the positioning of the fatty acid. However, the electron density for the region around the nitrogen is poor and does not allow for modelling of the fatty acid

Size distributions

The size distributions obtained from NNLS analyses were consistent with the cumulants results. For protein concentrations ranging from 10 mg/ml to 60 mg/ml, the intensity distributions were usually found to be monomodal for native (or control) and caprylated RNases, and trimodal for myristoylated and palmitoylated RNases. In the two last cases, two populations with diameters around 15 nm and 100 nm were consistently observed in addition to the diameter of 4 nm, already obtained for native or caprylated RNase A and corresponding to the monomer size. Some typical size distributions are shown in Fig. 5. Size distributions require extremely accurate data and resolution in particle size is limited by the ill-conditioning of the inversion of multi-exponential data (Finsy 1994). Also, owing to the dependence of scattering power, which, for small particles, is proportional to d^6, intensity distributions emphasize the presence of larger particles. Since the amount of information that can be extracted reliably was subject to uncertainty, no further investigations concerning changes in size or relative amounts of particles were attempted.

Discussion

Obtaining structural data for naturally occurring lipidated proteins is a difficult task owing to the hydrophobic character of the attached lipid chain which may hinder crystallization, if exposed to the solvent. To date, only the X-ray structure of native cAPK (Zheng et al. 1993) and the NMR

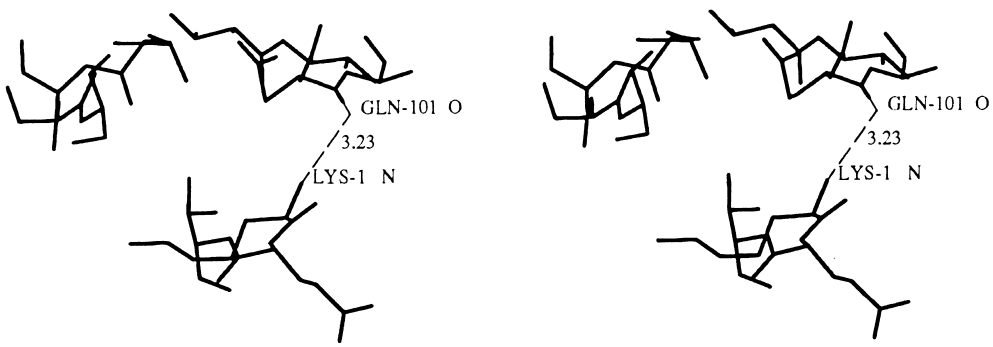

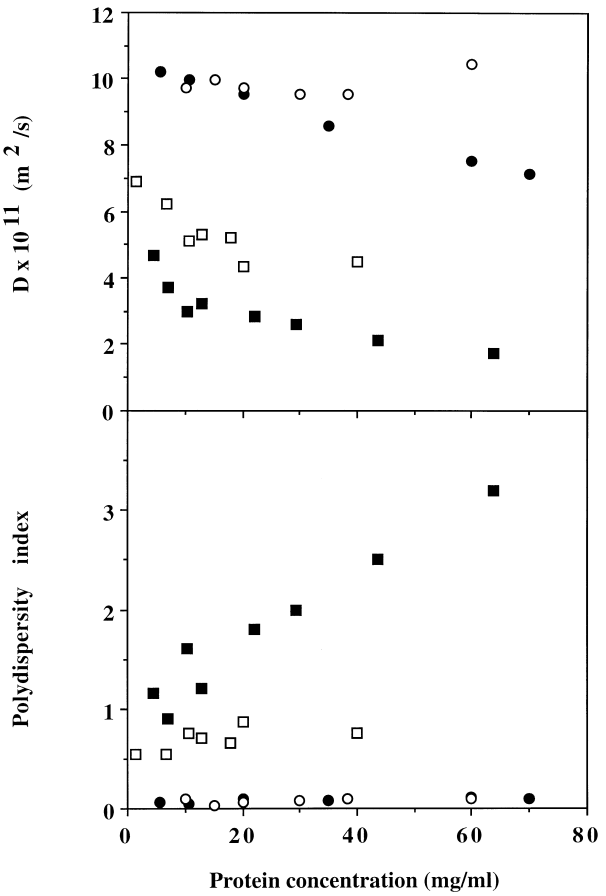

Fig. 4 Diffusion coefficient and polydispersity index obtained from analysis by the method of cumulants as a function of protein concentration; ○: unmodified RNase A (native or control); ●: caprylated RNase A; □: myristoylated RNase A; ■: palmitoylated RNase A. Experimental conditions: 50 mM sodium acetate, pH 5.1, 20 °C

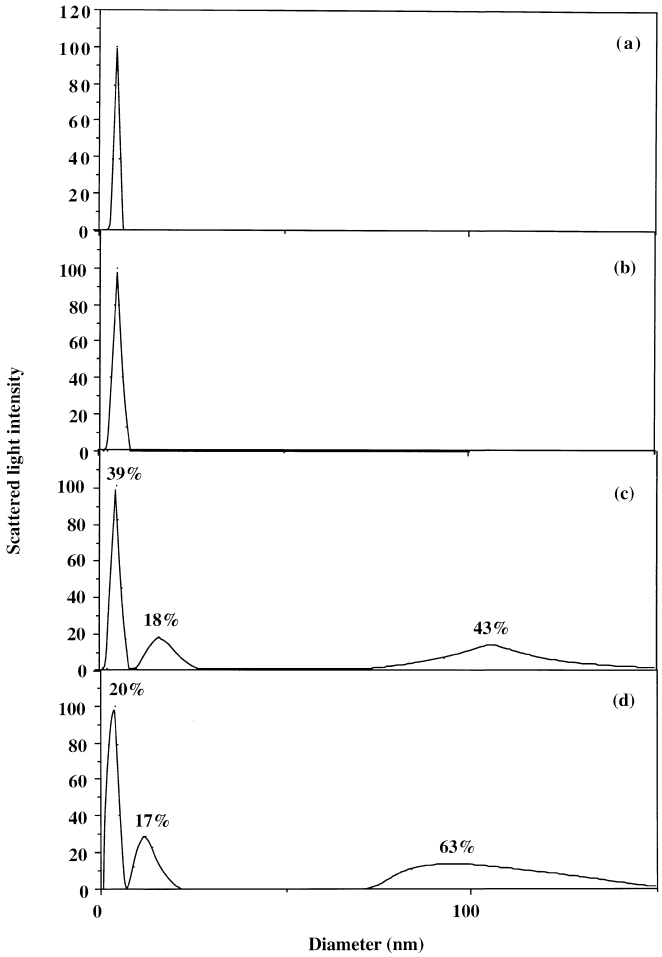

Fig. 5a–d Particle size distributions obtained from analysis with NNLS method. **a** control RNase A, 20 mg/ml; **b** caprylated RNase A, 20 mg/ml; **c** myristoylated RNase A, 20 mg/ml; **d** palmitoylated RNase A, 18 mg/ml. Relative light scattered intensities are indicated above the peaks. Other experimental conditions as in Fig. 4

structure of myristoylated calcium-free recoverin (Tanaka et al. 1995) have been determined. In both cases, the myristoyl group is buried in a hydrophobic pocket, unavailable for external interactions. In the present study, we used a chemically modified RNase A as a model to investigate the effect of acyl chain length on crystallization.

Conformation of the modified proteins

Taking into account the accessibilities and the pK values of the amino groups, we expected the α-amino group of lysine-1 to react faster than ε-amino groups with fatty acid chlorides. Chemical modifications of the amino groups of RNase A show preferential reaction sites at the α-amino group of lysine-1, the ε-amino group of lysine-1, the ε-amino group of lysine-41 and to a lesser extent, the ε-amino group of lysine-7 (Richards and Wyckoff 1971). Lysine-7 and lysine-41 belong to the active site and modification of either ε-amino-group would result in a significant loss of activity. All the acyl derivatives are fully active with enzymatic properties similar to those of native RNase A; moreover, they do not exhibit any significant Edman degradation. It can be concluded that, for our conditions, the modification of RNase A by fatty acid chlorides occurs at the α-amino group; it does not affect the catalytic activity of the protein, in agreement with the results of other modifications at the same site (Garel 1976).

The comparison of the refined structures of different RNase A models has revealed different positions of side-chain and main-chain atoms for Lys-1, suggesting a high flexibility for the N-terminal residue (Wlodawer et al. 1988). Therefore, a possible movement of the polypeptide chain in order to bury the fatty acid chain into a hydrophobic pocket could not be excluded. The crystal structure of caprylated RNase A indicates that no long-range effect on conformation can be ascribed to the presence of a covalently bound acyl chain; there is no conformational change of the polypeptide chain in order to accommodate the acyl chain. Similarly, the crystal structure of another chemical

derivative modified at the N-terminal lysine residue with a nucleotide revealed no change in the overall conformation of the protein (Boqué et al. 1994).

The lack of electron density for the capryl chain in the crystal structure suggests that the chain protudes into the solvent with a high degree of mobility. Neither the portion of the acyl chain near the site of covalent attachment nor the more distal part are immobilized. Whereas crystal packing is unaffected by the chemical modification, it creates a cavity large enough to accommodate the mobile capryl chain. The acyl group probably points away from the surface of the protein, as does the sugar residue attached at Asn 34 in RNase B, the glycosylated form of the protein (Williams et al. 1987). In contrast, the myristoyl and palmitoyl moieties, which probably also protude into the solvent, are too long to be accommodated by the crystal packing and prevent crystal formation. Moreover, self-association of protein molecules may impede crystallization (see below).

Probably owing to its high accessibility and mobility, Lys-1 is always involved in crystal packing contacts. In trigonal crystals of semi-synthetic RNase A, where one molecule is surrounded by five neighbours, three types of interfaces have been identified, with areas varying from 390 to 1860 $Å^2$ (Crosio et al. 1992). Lys-1 is involved in the smallest one, through a hydrogen bond also observed here. Therefore, the addition of a relatively short acyl chain (10 carbon atoms) to the N-terminal does not interfere with such a contact and does not interfere with crystal packing.

Implications for solubility

At pH 5.1, in the absence of salts, the polydispersity of the solutions and the dependence of the diffusion coefficient on protein concentration differ from one species to the other. For caprylated, as well as for native or control protein, the plot of the diffusion coefficient is linear and extrapolates to the monomer diffusion coefficient at infinite dilution (Boyer et al. 1996). The decreasing diffusion coefficient with increasing caprylated RNase A concentration indicates attractive interactions. However, distribution profiles do not reveal self-association. This attractive force, probably due to the extruding capryl chain, may explain why salt concentrations necessary for crystallizing the caprylated protein are lower than those used for the native form. Longer alkyl chains clearly enhance the tendency toward aggregation and attractive interactions between myristic and palmitic groups are sufficient to cause protein association. Distribution profiles reveal two sizes of aggregates: small aggregates with diameters around 15 nm and large aggregates with diameters one order of magnitude larger. A possible structure for the small aggregate would be a spherical micelle since such an arrangement leads to a soluble structure. The acylated protein may be considered as an amphiphilic molecule with a large polar head group compared to the saturated hydrocarbon chain of the fatty acyl chain. Above a critical concentration, amphiphiles present the ability to assemble into structures of finite size but the head volume and the chain length set limits on how the fluid chain can pack together. Amphiphiles with large head group area and small hydrocarbon volume lead to spherical micelles in water (Israelachvili 1985) with aggregation number insensitive to total concentration above the critical concentration. Assuming a maximum length of about 2 nm for the acyl chain and 4 nm diameter for the polar head, the corresponding diameter of a spherical micelle would be 12 nm, in agreement with the first aggregated population observed in the distributions. In such a case, an approximate number of 20 interacting monomeric units can be calculated from the hydrodynamic diameter of the supposed micelle. It is more difficult to imagine what species corresponds to the second aggregated population. We suspect the large aggregates, observed for both myristoyl- and palmitoyl-RNase A, to be associations between partly unfolded molecules and acylated proteins. Protein unfolding exposes hydrophobic patches which may lead to unspecific associations. In fact, the special experimental conditions used for the chemical reaction and the purification might destabilize the protein. Such a hypothesis would be supported by the fact that bimodal distributions with the same type of large aggregates were sometimes obtained for caprylated or control RNase A but they could be removed, as they appeared, by subsequent filtrations. Such numerous filtrations were impossible in the case of longer chains owing to the progressive loss of acylated protein, probably by adsorption to the filter.

Implications for function

The modified protein, with one acyl chain attached to its N-terminal group, mimics well many natural monoacylated proteins. Any exposed acyl group may mediate membrane binding by inserting into a lipid bilayer. There are several reports on the interaction of fatty acids with phospholipid vesicles. The binding energies of fatty acids and acylated peptides to phospholipid vesicles are found to increase linearly with the number of carbons in the lipid chain (Peitzsch and McLaughlin 1993), while the presence of only one acyl chain often appears not to be sufficient for a stable interaction. Portions of the polypeptide chain of an acylated protein may of course exhibit additional distinct interactions with the membrane bilayer: hydrophobic and electrostatic interactions may act together to anchor the protein to a membrane. In fact, several myristoylated proteins contain a cluster of basic residues that are supposed to bind to acidic phospholipids (Resh 1994). Also, protein-protein interactions between acylated proteins may favor the membrane attachment by increasing the number of acyl groups. The structure of rat ARF-1 suggests the possibility that ARF-1 could exist as a dimer while attached to the membrane and cycle between monomeric and dimeric states as well as between GDP and GTP-bound states (Greasly et al. 1995). With both acyl groups located on a common face, the structure of heterotrimeric G proteins would be consistent with a cooperative insertion into the lipid bilayer (Lambright et al. 1996).

The membrane binding may obviously be modulated by other partners that can bind the acyl group in the aqueous phase. The present results suggest that, among several factors that could perturb the membrane bound/aqueous partitioning of acylated proteins, self-association of polypeptides through acyl group interaction must be considered. It must be pointed out that naturally occurring acyl chains are at least 14 carbon atoms long. Interestingly, based on our light scattering results, such a length appears also as a minimum length to create sufficient attractive forces to induce protein aggregation. In this sense, two-dimensional nuclear magnetic resonance techniques have shown that N-myristoylated oligopeptides are capable of self-aggregation owing to their lipid component (Sankaram 1994). Future strategies concerning acylated proteins will need to address whether self-associating properties may play a role in regulating their overall function.

Conclusion

In summary, we have shown that the chemical attachment of one fatty acid moiety to N-terminal lysine does not have any influence on RNase A conformation, giving as a good model for studying the effects of acylation on protein solubility and crystallization. Dynamic light scattering results indicate that, while native and caprylated RNases remain monomeric in concentrated solutions, acylation with longer chain lengths results in the formation of aggregates. Such a self-association might explain why myristoylated and palmitoylated RNases do not crystallize.

Acknowledgements The support of Dr. J.-M. Lhoste is gratefully acknowledged. We are indebted to Dr. B. Lagoutte (Département de Biologie Cellulaire et Moléculaire, URA CNRS 1290, Commissariat à l'Energie Atomique, Centre d'Etudes de Saclay, 91191 Gif-sur-Yvette, France) for the NH_2-terminal sequence analyses and H. Adenier (UTC) for the mass spectrometry measurements. We thank Dr. C. Le Grimellec for stimulating discussions.

References

Baudet-Nessler S, Jullien M, Crosio M-P, Janin J (1993) Crystal structure of a fluorescent derivative of RNase A. Biochemistry 32:8557–8464

Boqué L, Coll MG, Vilanova M, Cuchillo CM, Fita I (1994) Structure of ribonuclease A derivative II at 2.1 Å resolution. J Biol Chem 269:19707–19712

Boyer M, Roy M-O, Jullien M (1996) Dynamic light scattering study of precrystallizing ribonuclease solutions. J Crystal Growth 167:212–220

Brünger AT (1992) X-PLOR Version 3.1. A system for X-ray crystallography and NMR. Yale University Press, New Haven

Camilleri P, Haskins NJ, Rudd PM, Saunders MR (1993) Applications of electrospray mass spectrometry to studies on the structural properties of Ribonuclease A and Ribonuclease B. Rapid Commun. Mass Spec 7:332–335

Casey PJ (1995) Protein lipidation in cell signaling. Science 268:221–225

Crook EM, Mathias AP, Rabin BR (1960) Spectrophotometric assay of bovine pancreatic ribonuclease by the use of cytidine 2′:3′-phosphate. Biochem J 74:234–238

Crosio M-P, Janin J, Jullien M (1992) Crystal packing in six crystal forms of pancreatic ribonuclease. J Mol Biol 228:243–251

Del Mel VSJ, Martin PD, Doscher MS, Edwards BFP (1992) Structural changes that accompany the reduced catalytic efficiency of two semisynthetic ribonuclease analogs. J Biol Chem 267: 247–256

Finsy R (1994) Particle sizing by quasi-elastic light scattering. Adv Colloid Interface Sci 52:79–143

Garavito RM, Picot D (1990) The art of crystallizing membrane proteins. Methods: a companion to methods in enzymology 1: 57–69

Garel J-R (1976) PK changes of ionizable reporter groups as an index of conformational changes in proteins. Eur J Biochem 70:179–189

Greasly SE, Jhoti H, Teahan C, Solari R, Fensome A, Thomas GMH, Cockroft S, Bax B (1995) The structure of rat ADP-ribosylation factor-1 (ARF-1) complexed to GDP determined from two different crystal forms. Nature Struct Biol 2:797–806

Israelachvili JN (1985) Intermolecular and surface forces. Academic Press, London

Jones TA, Kjeldgaard M (1992) O – the manual. Uppsala, Sweden

Kabanov AV, Levashov AV, Alakhov VY (1989) Lipid modification of proteins and their membrane transport. Protein Eng 3:39–42

Kabsch W (1988) Evaluation of single-crystal X-ray diffraction data from a position-sensitive detector. J Appl Cryst 21:916–924

Koppel DE (1972) Analysis of macromolecular polydispersity in intensity correlation spectroscopy: the method of cumulants. J Chem Phys 57:4814–4820

Lambright DG, Sondek J, Bohm A, Skiba NP, Hamm HE, Sigler PB (1996) The 2.0 Å crystal structure of a heterotrimeric G protein. Nature 379:311–319

Marschall CJ (1993) Protein prenylation: a mediator of protein-protein interactions. Science 259:1865–1866

McPherson A, Malkin AJ, Kuznetsov YG (1995) The science of macromolecular crystallization. Structure 3:759–768

Morrison ID, Grabowski EF, Herb CA (1985) Improved techniques for particle size determination by quasi-elastic light scattering. Langmuir 1:496–501

Peitzsch RM, McLaughlin S (1993) Binding of acylated peptides and fatty acids to phospholipid vesicles: pertinence to myristoylated proteins. Biochemistry 32:10436–10443

Pusey PN, Tough RJA (1985) Particle interactions. In: Pecora R (ed) Dynamic light scattering. Plenum, New York, pp 85–179

Resh MD (1994) Myristylation and palmitylation of Src family members: the fats of the matter. Cell 76:411–413

Richards FM, Wyckoff HW (1971) Bovine pancreatic ribonuclease. In: Boyer P (ed) The enzymes 3rd edn, vol 4. Academic Press, New York, pp 647–806

Robert S, Domurado D, Thomas D, Chopineau J (1993) Fatty acid acylation of RNase A using reversed micelles as microreactors. Biochem Biophys Res Commun 196:447–454

Sankaram MB (1994) Membrane interaction of small N-myristoylated peptides: implications for membrane anchoring and protein-protein association. Biophys J 67:105–112

Tanaka T, Ames JB, Harvey TS, Stryer L, Ikura M (1995) Sequestration of the membrane-targeting myristoyl group of recoverin in the calcium-free state. Nature 376:444–447

Williams RL, Greene SM, McPherson A (1987) The crystal structure of ribonuclease B at 2.5 Å resolution. J Biol Chem 262:16020–16031

Wlodawer A, Svensson LA, Sjölin L, Gilliland GL (1988) Structure of phosphate-free ribonuclease A refined at 1.26 Å. Biochemistry 27:2705–2717

Zegers I, Maes D, Dao-Thi M-H, Poortmans F, Palmer R, Wyns L (1994) The structure of RNase A complexed with 3′-CMP and d(CpA): active site conformation and conserved water molecules. Protein Sci 3:2322–2339

Zheng I, Knighton DR, Xuong NH, Taylor SS, Sowadski JM, Ten Eyck LF (1993) Crystal structures of the myristylated catalytic subunit of cAMP-dependent protein kinase reveal open and closed conformations. Protein Sci 2:1559–1573